

# Multivariable Process Control: Decentralized, Decoupling, or Sparse?

Yuling Shen,<sup>†</sup> Wen-Jian Cai,<sup>\*,‡</sup> and Shaoyuan Li<sup>†</sup>

Department of Automation, Shanghai Jiao Tong University, 800 Dongchuan Road, Minhang, Shanghai 200240, China, and School of Electrical and Electronic Engineering, Nanyang Technological University, Singapore 639798, Singapore

In this article, a systematic approach is proposed to design PI-/PID-based multivariable control systems in which the designs and analyses of decentralized, decoupling, and sparse control schemes are all treated under a unified framework. First, based on the relative normalized gain array (RNGA), a best loop pairing is obtained using the RGA (relative gain array)–Nederlinski index (NI)–RNGA rules. The index matrix is then calculated, and the control structure is determined according to a selection criterion. Finally, the selected loop controllers are independently designed based on equivalent transfer functions. The effectiveness of the proposed design approach is verified by analysis of several multivariable industrial processes, demonstrating that the selected control structure results in better overall system performance.

## 1. Introduction

Energy and material recycling design and tight control requirements for modern industrial processes justify the need to implement multivariable control schemes. However, multivariable controllers are much more difficult to design and implement than their single-input–single-output (SISO) counterparts, because of the existence of interactions among the loops. Even though several model predictive control (MPC) schemes have emerged in the process control industry to handle constraints and interactions, their computational complexity makes them more suitable for a higher level in the control structure, whereas control schemes based on proportional–integral (PI)/proportional–integral–derivative (PID) controllers are still widely used at the lower levels for regulating controls. As such, research on PI-/PID-based multivariable control system analysis and design has received great interest from academia and industry alike.

PI-/PID-based control can generally be classified into two main groups: decentralized control and decoupling control. In decentralized control, a multivariable process is decomposed into multiple single-input–single-output (SISO) processes, and the controllers are designed for each individual loop by taking the loop interactions into account. So far, decentralized control is still the dominant control scheme in multivariable control because it has many advantages, such as flexibility in operation, failure tolerance, and simplified design and tuning. Over the years, several methods for decentralized control system design have been proposed, including detuning factor methods,<sup>1–3</sup> sequential loop closing methods,<sup>4,5</sup> and equivalent transfer function methods.<sup>6,7</sup> Decentralized control can generally work well when loop interactions are modest. However, when the processes are closely coupled, it inevitably leads to performance degradation compared to full-dimensional control schemes, as the tuning of the loop controller is aimed at a compromise between improving system performance and conquering loop interactions.

On the other hand, decoupling control schemes are often employed for those processes that are closely coupled and/or require tight control. In this type of control scheme, by first

eliminating the effects of the undesirable cross-couplings, the process can then be treated as multiple single loops, and less-conservative single-loop PID control design methods can be directly applied. Several decoupling control schemes are currently available, such as ideal decoupling,<sup>8</sup> simplified decoupling,<sup>9</sup> inverted decoupling,<sup>10</sup> decoupling via linear matrix inequality (LMI),<sup>11</sup> decoupling-based step/relay test,<sup>12,13</sup> and normalized decoupling.<sup>14,15</sup> Even though decoupling control can provide better performance than decentralized control schemes for closely coupled processes, it can result in very complex structures, especially when a multivariable process is of high dimension, making it impossible to implement in practice.

To compromise between the two control schemes, sparse control structures were proposed, including “block diagonal control” and “triangular control” structures.<sup>16–19</sup> By adding some extra off-diagonal controllers, sparse control is simpler than full multi-input–multi-output (MIMO) control, but it is able to achieve superior performance compared to decentralized control if it is properly designed. However, the design of sparse control is not as simple as it appears to be because two important but difficult issues need to be resolved: (1) Which loops should be controlled other than the diagonal ones? The consideration should be based on a balance of control structure simplicity, system performance, and robustness. (2) How should the controllers be designed? Design of a controller for one loop is dependent on all other loop controllers because of the existence of interactions. Ideally, a good design should be simple for practical engineers while taking the loop interactions into consideration. Unfortunately, these two issues remain unsolved, which has limited algorithm development for and real-world applications of sparse control.

In this article, a systematic approach is proposed to design PI-/PID-based multivariable control systems in which decentralized, decoupling, and sparse control schemes are all placed under a unified framework. The main features of the approach include the following: 1) By employing the concept of relative normalized gain array (RNGA),<sup>20</sup> an interaction index is defined to evaluate the seriousness of the interactions of the off-diagonal elements. (2) A control structure selection criterion is proposed through an analysis of relative gain and relative average time constant, as well as engineering experience. (3) The process equivalent transfer functions (ETFs)<sup>21</sup> when other loops are closed are derived based on the relative gain and relative average

\* To whom correspondence should be addressed. Tel.: +65 6790 6862. Fax: +65 6793 3318. E-mail: ewjcai@ntu.edu.sg.

<sup>†</sup> Shanghai Jiao Tong University.

<sup>‡</sup> Nanyang Technological University.

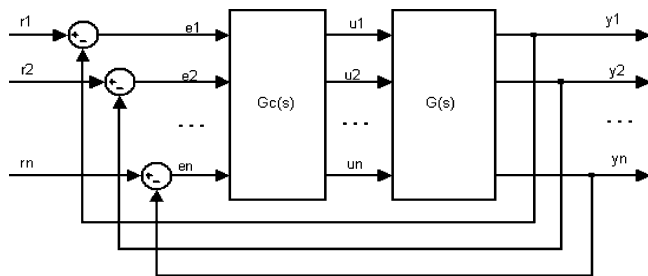


Figure 1. Closed-loop multivariable control system.

time constant of each loop for the control system design. (4) An independent design method is proposed for control system design such that the controllers can be designed independently of each other. By this design approach, the conversion between decentralized control, decoupling control, and sparse control can be simply achieved by adding or dropping corresponding controllers. The method is simple, straightforward, and easy to understand and implement. Several multivariable industrial processes with different interaction characteristics are employed to demonstrate the design procedure, as well as the simplicity and effectiveness of the design method.

## 2. Preliminaries

Consider an open-loop stable  $n \times n$  multivariable system as shown in Figure 1, where  $r_i$ ,  $i = 1, 2, \dots, n$ , represents the reference inputs;  $u_i$ ,  $i = 1, 2, \dots, n$ , represents the manipulated variables; and  $y_i$ ,  $i = 1, 2, \dots, n$ , represents the system outputs.  $\mathbf{G}(s)$  is the process transfer function matrix with compatible dimensions, described by

$$\mathbf{G}(s) = \begin{bmatrix} g_{11}(s) & g_{12}(s) & \dots & g_{1n}(s) \\ g_{21}(s) & g_{22}(s) & \dots & g_{2n}(s) \\ \vdots & \vdots & \ddots & \vdots \\ g_{n1}(s) & g_{n2}(s) & \dots & g_{nn}(s) \end{bmatrix} \quad (1)$$

Without loss of generality, the elements in the transfer function matrix can be considered first-order plus dead time (FOPDT)

$$g_{ij}(s) = \frac{k_{ij}}{\tau_{ij}s + 1} e^{-\theta_{ij}s} \quad (2)$$

for  $i, j = 1, 2, \dots, n$ , where  $k_{ij}$ ,  $\tau_{ij}$ , and  $\theta_{ij}$  are the process open-loop gain, time constant, and dead time, respectively. Because high-order transfer function elements can be simplified by either analytical or empirical methods,<sup>22,23</sup> FOPDT models will be used for interaction analysis and control system design for simplicity.

Before introducing the main results of this work, we first present some concepts that are important to our later development.

**2.1. Normalized Gain and Relative Normalized Gain Array (RGA).** In control system configuration, two factors in the open-loop transfer functions affect the loop pairing decision and should be focused on when considering the effect of interactions: steady-state information, because the steady-state gain of the transfer function  $g_{ij}(s)$  reflects the effect of manipulated variable  $u_j$  on controlled variable  $y_i$  when the system is stable, and transient information, as the transient information of the transfer function  $g_{ij}(s)$  is accountable for the sensitivity of the controlled variable  $y_i$  to manipulated variable  $u_j$  and, consequently, the promptness of a particular output response to an input and the ability to reject the interactions from other loops.

Hence, it is desired that the control structure can be configured based on an effective evaluation of control-loop interactions in terms of both steady-state and transient information. The steady-state information can be easily extracted from the process steady-state gain matrix, whereas the dynamic information can be obtained from the process average residence time,  $\tau_{ar,ij}$ , defined as the time constant plus dead time of the transfer function. For FOPDT processes, the average residence time  $\tau_{ar,ij}$  can be obtained as

$$\tau_{ar,ij} = \tau_{ij} + \theta_{ij} \quad (3)$$

A smaller  $\tau_{ar,ij}$  value indicates that the transfer function has a faster response to the inputs and disturbances, whereas a larger  $\tau_{ar,ij}$  value indicates slower process dynamics.

To use both steady-state gain and average residence time for interaction measuring and loop pairing, we defined the normalized gain  $k_{N,ij}$  for a particular transfer function  $g_{ij}(s)$  as<sup>16</sup>

$$k_{N,ij} = \frac{g_{ij}(j0)}{\tau_{ar,ij}} \quad (4)$$

and for all elements, the normalized gain matrix  $\mathbf{K}_N$  is

$$\mathbf{K}_N = [k_{N,ij}]_{n \times n} = \mathbf{G}(j0) \odot \mathbf{T}_{ar} \quad (5)$$

where  $\mathbf{T}_{ar} = [\tau_{ar,ij}]_{n \times n}$  and  $\odot$  indicates element-by-element division.

When the relative normalized gains are calculated for all input/output combinations of a multivariable process, the result is an array with a form similar to that of the relative gain array (RGA), called the RGA,  $\mathbf{\Lambda}_N = [\lambda_{N,ij}]_{n \times n}$ , which can be calculated as

$$\mathbf{\Lambda}_N = \mathbf{K}_N \otimes \mathbf{K}_N^{-T} \quad (6)$$

**2.2. Loop Pairing Rules Based on RGA–NI–RGA.** For the Niederlinski index (NI), given as

$$NI = \frac{|\mathbf{G}(0)|}{\prod_{i=1}^n g_{ii}(0)} \quad (7)$$

where  $|\mathbf{G}(0)|$  denotes the determinant of matrix  $\mathbf{G}(0)$ , RGA and NI tools can provide sufficient conditions to filter out the structurally unstable control configurations. That is, the RGA and NI tools can be used to eliminate those structures with unstable pairing options, whereas the RGA can find the pairing with the best overall performances. Thus, the RGA–NI–RGA-based control configuration criterion is given as follows:<sup>20</sup>

Manipulated and controlled variables in a decentralized control system should be paired in such a way that (i) all paired RGA elements are positive, (ii) the NI is positive, (iii) the paired RGA elements are closest to 1.0, and (iv) large RGA elements are avoided. Because this pairing criterion takes the RGA, RGA, and NI into consideration, it offers important insights into the issue of control structure selection. The RGA is used to measure the loop interactions over the whole frequency range, whereas the RGA and NI are used as sufficient conditions to rule out closed-loop unstable pairings.

**2.3. Equivalent Transfer Function (ETF).** To reveal the model relations between the conditions under which all loops are open and all loops are closed, the relative average resident time (RART),  $\gamma_{ij}$ , was introduced. It is defined as the ratio of loop  $y_i-u_j$  average resident times between when other loops are closed and when other loops are open<sup>14</sup>

$$\gamma_{ij} \triangleq \frac{\hat{\tau}_{ar,ij}}{\tau_{ar,ij}} \quad i, j = 1, 2, \dots, n \quad (8)$$

where  $\hat{\tau}_{ar,ij}$  is the average resident time when other loops are closed.

When RARTs are calculated for all average resident times of a transfer function matrix, the result is an array with a form similar to that of RNGA, called the relative average residence time array (RARTA), which is calculated as

$$\mathbf{\Gamma} \triangleq \mathbf{\Lambda}_N \odot \mathbf{\Lambda}$$

$$= \begin{bmatrix} \lambda_{N,11} & \lambda_{N,12} & \dots & \lambda_{N,1n} \\ \lambda_{N,21} & \lambda_{N,22} & \dots & \lambda_{N,2n} \\ \vdots & \vdots & \ddots & \vdots \\ \lambda_{N,n1} & \lambda_{N,n2} & \dots & \lambda_{N,nn} \end{bmatrix} \otimes \begin{bmatrix} \lambda_{11}^{-1} & \lambda_{12}^{-1} & \dots & \lambda_{1n}^{-1} \\ \lambda_{21}^{-1} & \lambda_{22}^{-1} & \dots & \lambda_{2n}^{-1} \\ \vdots & \vdots & \ddots & \vdots \\ \lambda_{n1}^{-1} & \lambda_{n2}^{-1} & \dots & \lambda_{nn}^{-1} \end{bmatrix} \quad (9)$$

From the definition of the RARTA, the closed-loop average residence time can then be written as

$$\begin{aligned} \hat{\tau}_{ar,ij} &= \gamma_{ij} \tau_{ar,ij} = \gamma_{ij} \tau_{ij} + \gamma_{ij} \theta_{ij} \\ &\triangleq \hat{\tau}_{ij} + \hat{\theta}_{ij} \end{aligned} \quad (10)$$

By assigning the equivalent transfer functions (ETFs) when other loops are closed to have the same structure as the open-loop transfer functions, the ETFs can be approximated in terms of relative gains and relative average resident times when the control system is closed. The ETFs for FOPDT processes are given as

$$\hat{g}_{ij}(s) = \hat{k}_{ij} \frac{1}{\hat{\tau}_{ij}s + 1} e^{-\hat{\theta}_{ij}s} = \frac{k_{ij}}{\lambda_{ij} \gamma_{ij} \tau_{ij}s + 1} e^{-\gamma_{ij} \theta_{ij}s} \quad (11)$$

### 3. Control Structure Selection

Generally, a multivariable process can be controlled by decentralized, decoupling, or sparse control schemes. Each of these types of control is briefly discussed here.

Decentralized control has a diagonal controller structure

$$\mathbf{G}_c(s) = \begin{bmatrix} g_{c1}(s) & 0 & \dots & 0 \\ 0 & g_{c2}(s) & \dots & 0 \\ \vdots & \vdots & \ddots & \vdots \\ 0 & 0 & \dots & g_{cn}(s) \end{bmatrix} \quad (12)$$

and is the simplest control structure for multivariable processes.

Decoupling control is a full control structure

$$\mathbf{G}_c(s) = \begin{bmatrix} g_{c,11}(s) & g_{c,12}(s) & \dots & g_{c,1n}(s) \\ g_{c,21}(s) & g_{c,22}(s) & \dots & g_{c,2n}(s) \\ \vdots & \vdots & \ddots & \vdots \\ g_{c,n1}(s) & g_{c,n2}(s) & \dots & g_{c,nn}(s) \end{bmatrix} \quad (13)$$

that first eliminates the effects of the undesirable cross-couplings using off-diagonal controllers, such that the process can be treated as multiple single loops, and less-conservative single-loop PID control design methods can be directly applied by diagonal controllers.

In sparse control, a sparse controller structure

$$\mathbf{G}_c(s) = \begin{bmatrix} g_{c,11}(s) & \kappa_{12} & \dots & \kappa_{1n} \\ \kappa_{21} & g_{c,22}(s) & \dots & \kappa_{2n} \\ \vdots & \vdots & \ddots & \vdots \\ \kappa_{n1} & \kappa_{n2} & \dots & g_{c,nn}(s) \end{bmatrix} \quad (14)$$

where  $\kappa_{ij}$  is the off-diagonal controller index

$$\kappa_{ij} = \begin{cases} 1, & g_{c,ij}(s) \\ 0, & \text{no controller} \end{cases} \quad \text{for } i \neq j; i, j = 1, 2, \dots, n \quad (15)$$

The advantages of sparse control lie in the fact that the control performance can be improved with limited structure complexity while still preserving control system integrity.

To unify the control structure selection procedure, we first put the selected pairs on the diagonal positions by column transformation of both the RNGA and the transfer function matrix, and we then rationalize the matrix by making all diagonal elements equal to 1, which can be calculated by defining an “interaction index”,  $\mathbf{B} = [\beta_{ij}]_{n \times n}$ , where

$$\beta_{ij} = \left| \frac{\lambda_{N,ij}}{\lambda_{N,ii}} \right| = \left| \frac{\lambda_{ij} \gamma_{ij}}{\lambda_{ii} \gamma_{ii}} \right| \quad (16)$$

To analyze the effects of  $\beta_{ij}$  on the selection of  $\kappa_{ij}$ , consider two extreme cases:

(1) If  $\beta_{ij}$ ,  $j \neq i$ , is very small, then this implies that either  $\lambda_{ij}/\lambda_{ii}$  is very small or  $\gamma_{ij}/\gamma_{ii}$  is very large.  $\lambda_{ij}/\lambda_{ii}$  being very small would mean that  $k_{ij}$  is very small compared with  $k_{ii}$ . In this case, the input  $u_j$  has very little influence on  $y_i$ . On the other hand,  $\gamma_{ij}/\gamma_{ii}$  being very small means that  $\tau_{ar,ij}$  is very small compared with  $\tau_{ar,ii}$ , the  $i$ - $j$  loop reacts very rapidly, and the effect of the fast loop appears as a high-frequency disturbance that can be effectively filter out by the relatively slow paired control loop.

(2) If  $\beta_{ij}$ ,  $j \neq i$ , is very large, then this implies that either  $\lambda_{ij}/\lambda_{ii}$  is very large or  $\gamma_{ij}/\gamma_{ii}$  is very small. If  $\lambda_{ij}/\lambda_{ii}$  is very large, then, with this loop included, the steady-state gain matrix is nearly singular. The system is very sensitive to modeling errors, so that small modeling errors will be magnified into very large errors in  $y_i$  and a small change in controller output  $u_j$  will also result in large errors in  $y_i$ . Control will be difficult to achieve for such a loop, and it will also be very sensitive to modeling errors. On the other hand, the fact that  $\gamma_{ij}/\gamma_{ii}$  is very large means that  $\tau_{ar,ij}$  is very large compared with  $\tau_{ar,ii}$ , such that the loop reacts very slowly. The effect of the slow loop appears as a constant disturbance that can be effectively rejected by the paired loop controllers.

Based on the preceding analysis of the process characteristics, the economic value of improved control, and the reasonable computing and process control resources, we propose the following control selection criterion for  $\kappa_{ij}$  as general guideline for engineering applications

$$\kappa_{ij} = \begin{cases} 1, & 0.15 \leq \beta_{ij} \leq 8 \\ 0, & \text{otherwise} \end{cases} \quad \text{for } i \neq j; i, j = 1, 2, \dots, n \quad (17)$$

Because the RNGA for a  $2 \times 2$  system is symmetric, it should be controlled by either a decentralized or decoupling control scheme, whereas for  $n > 2$ , decentralized, decoupling, and sparse control schemes all can be applied, at least in theory. However, because a process suitable for full decoupling control can seldom be found, a decentralized or sparse control scheme is generally more appropriate.

### 4. Independent Design

For a closed-loop-controlled MIMO system, it is desirable that the forward transfer function be of the form

$$\mathbf{G}(s) \mathbf{G}_c(s) \approx \frac{\mathbf{I}}{s} \quad (18)$$

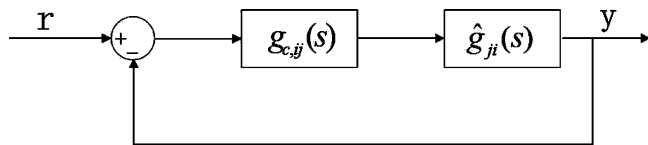


Figure 2. Block diagram of the independent design method.

such that the sensitivity and complementary sensitivity functions approach 0 and 1, respectively.

From the relationship between  $G^{-1}(s)$  and the ETF matrix, we have<sup>14</sup>

$$\mathbf{G}^{-1}(s) = \hat{\mathbf{G}}^T(s) = \begin{bmatrix} \hat{g}_{11}^{-1}(s) & \hat{g}_{21}^{-1}(s) & \cdots & \hat{g}_{n1}^{-1}(s) \\ \hat{g}_{12}^{-1}(s) & \hat{g}_{22}^{-1}(s) & \cdots & \hat{g}_{n2}^{-1}(s) \\ \vdots & \vdots & \ddots & \vdots \\ \hat{g}_{1n}^{-1}(s) & \hat{g}_{2n}^{-1}(s) & \cdots & \hat{g}_{nn}^{-1}(s) \end{bmatrix} \quad (19)$$

Substituting 19 into eq 18 gives

$$\mathbf{G}_c(s) \approx \mathbf{G}^{-1}(s) \frac{\mathbf{I}}{s} = \begin{bmatrix} \frac{\hat{g}_{11}^{-1}(s)}{s} & \frac{\hat{g}_{21}^{-1}(s)}{s} & \cdots & \frac{\hat{g}_{n1}^{-1}(s)}{s} \\ \frac{\hat{g}_{12}^{-1}(s)}{s} & \frac{\hat{g}_{22}^{-1}(s)}{s} & \cdots & \frac{\hat{g}_{n2}^{-1}(s)}{s} \\ \vdots & \vdots & \ddots & \vdots \\ \frac{\hat{g}_{1n}^{-1}(s)}{s} & \frac{\hat{g}_{2n}^{-1}(s)}{s} & \cdots & \frac{\hat{g}_{nn}^{-1}(s)}{s} \end{bmatrix}$$

Define an error function as

$$\mathbf{E}(s) = \mathbf{G}_c(s) - s^{-1} \hat{\mathbf{G}}^T(s) \quad (20)$$

To minimize the error function, we define the objective function

$$J = \min |E(s)| = \min \sum_{i=1}^n \sum_{j=1}^n |\mathbf{G}_c(s) - s^{-1} \hat{\mathbf{G}}^T(s)|_{ij} \quad (21)$$

where the subscript  $ij$  indicates the element in the  $i$ th row and  $j$ th column of  $[\cdot]$ .

Because

$$|\mathbf{G}_c(s) - s^{-1} \hat{\mathbf{G}}^T(s)|_{ij} \approx \begin{cases} |g_{c,ij} - s^{-1} \hat{g}_{ji}|, & g_{c,ij}(s) \neq 0 \\ |s^{-1} \hat{g}_{ji}|, & g_{c,ij}(s) = 0 \end{cases} \quad (22)$$

the minimization of  $J$  requires that  $g_{c,ij}(s)$  be determined by

$$g_{c,ij}(s) - s^{-1} \hat{g}_{ji}^{-1}(s) = 0 \Rightarrow g_{c,ij}(s) \hat{g}_{ji}(s) = \frac{1}{s} \quad (23)$$

Imagine that  $g_{c,ij}(s) \hat{g}_{ji}(s)$  is the forward transfer function of an artificial closed control system as shown in Figure 2. Then,  $g_{c,ij}(s) \hat{g}_{ji}(s) = 1/s$  is the ideal control performance target for the loop, and the controller design is totally independent of the other loops.

In designing controllers for multivariable control systems, the closed-loop integrity is very important to guarantee that the overall system remains stable regardless of the removal or insertion of control loops. The integrity requires that each individual loop controller be no more aggressive than the original single-loop controller without interactions. For different combinations of  $\hat{\lambda}_{ij}$  and  $\hat{\gamma}_{ij}$ , general rules for the design of each loop controller are discussed as follows:

**Case 1:**  $|\hat{\lambda}_{ij}| \leq 1$ ,  $\hat{\gamma}_{ij} \geq 1$ .  $|\hat{\lambda}_{ij}| \leq 1$  means that the retaliatory effect when all the other loops are closed magnifies the effect of  $u_j$  on  $y_i$ , so the controller gain should be reduced accordingly to ensure system stability. In this case

$$\hat{k}_{ij} = \frac{k_{ij}}{\lambda_{ij}} \quad (24)$$

$\lambda \hat{\gamma}_{ij} \geq 1$  implies that the average residence time when the other loops are closed is not less than that when the other loops are open. The enlarged residence time will make the critical frequency shift to the left and reduce the phase margin. In this case

$$\hat{\tau}_{ar,ij} = \gamma_{ij} \tau_{ar,ij} \quad (25)$$

**Case 2:**  $|\hat{\lambda}_{ij}| > 1$ ,  $\hat{\gamma}_{ij} < 1$ .  $|\hat{\lambda}_{ij}| > 1$  indicates that the retaliatory effect when all other loops are closed reduces the effect of  $u_j$  on  $y_i$ . Because the controller gain cannot be enlarged for better performance because of system integrity considerations, no magnitude detuning for gain is needed. If  $\hat{\lambda}_{ij} < 0$ , then the sign of the steady-state gain is still supposed to be changed. In this case

$$\hat{k}_{ij} = k_{ij} \quad (26)$$

$\hat{\gamma}_{ij} < 1$  means that the average residence time when the other loops are closed is less than that when the other loops are open. The reduced residence time will make the critical frequency shift to the right and enlarge the phase margin. In this case, by considering system integrity, one obtains

$$\hat{\tau}_{ar,ij} = \tau_{ar,ij} \quad (27)$$

**Case 3:**  $|\hat{\lambda}_{ij}| \leq 1$ ,  $\hat{\gamma}_{ij} < 1$ .  $|\hat{\lambda}_{ij}| \leq 1$  is the same as in case 1, eq 23.

$\hat{\gamma}_{ij} < 1$  is the same as in case 2, eq 27.

**Case 4:**  $|\hat{\lambda}_{ij}| > 1$ ,  $\hat{\gamma}_{ij} \geq 1$ .  $|\hat{\lambda}_{ij}| > 1$  is the same as in case 2, eq 26.

$\hat{\gamma}_{ij} \geq 1$  is the same as in case 1, eq 25.

In summary, the integrity of sparse control can be preserved if the ETFs for controller design are updated as

$$\hat{k}_{ij} = \begin{cases} k_{ij}/\lambda_{ij}, & |\lambda_{ij}| < 1 \\ k_{ij}, & |\lambda_{ij}| \geq 1 \end{cases} \quad (28)$$

$$\hat{\tau}_{ar,ij} = \begin{cases} \gamma_{ij} \tau_{ar,ij} = \gamma_{ij} \tau_{ij} + \gamma_{ij} \theta_{ij}, & \gamma_{ij} > 1 \\ \tau_{ar,ij}, & 0 < \gamma_{ij} \leq 1 \end{cases} \quad (29)$$

Because perfect control is impossible, a PI/PID controller can be used to design  $g_{c,ij}(s)$  such that the closed loop of  $g_{c,ij}(s) \hat{g}_{ji}(s)$  has good dynamic properties. Under the gain and phase margin (GPM) design method, the loop forward transfer function is usually expressed as

$$g_{c,ij}(s) \hat{g}_{ji}(s) = \frac{k_{P,ij}}{s} e^{-L_{ij}s} \quad (30)$$

Let the PID controller be of the form

$$g_{c,ij}(s) = k_{P,ij} + \frac{k_{I,ij}}{s} + k_{D,ij}s \quad (31)$$

The ETFs together with the PID controller parameters for FOPDT are summarized for different combinations of  $\lambda_{ij}$  and  $\gamma_{ij}$  in Table 1.

**Remark 1.** If the loop transfer function has a high  $D/\tau$  ratio, the GPM method will result in a very aggressive PI/PID controller and deteriorate the whole stability. In such a case, internal model control (IMC)—Maclaurin is recommended for



**Table 1.** ETFs and PI Parameters for FOPDT Process

| mode  | $\hat{g}_{ij}(s)$  | $k_{p,ij}$  | $k_{i,ij}$   |
|---|--|---|--|
| $ \lambda_{ij}  < 1, 0 < \gamma_{ij} \leq 1$    | $\frac{k_{ij}}{\lambda_{ij}\tau_{ij}s + 1} e^{-\theta_{ij}s}$  | $\frac{\pi\lambda_{ij}T_{ij}}{2A_m\theta_{ij}k_{ij}}$ | $\frac{\pi\lambda_{ij}}{2A_m\theta_{ij}k_{ij}}$            |
| $ \lambda_{ij}  < 1, \gamma_{ij} > 1$           | $\frac{k_{ij}}{\lambda_{ij}\gamma_{ij}T_{ij}s + 1} e^{-\gamma_{ij}\theta_{ij}s}$                     | $\frac{\pi\lambda_{ij}T_{ij}}{2A_m\theta_{ij}k_{ij}}$ | $\frac{\pi\lambda_{ij}}{2A_m\gamma_{ij}\theta_{ij}k_{ij}}$ |
| $ \lambda_{ij}  \geq 1, \gamma_{ij} > 1$        | $\frac{\text{sign}(\lambda_{ij}) \cdot k_{ij}}{\gamma_{ij}T_{ij}s + 1} e^{-\gamma_{ij}\theta_{ij}s}$ | $\frac{\pi T_{ij}}{2A_m\theta_{ij}k_{ij}}$            | $\frac{\pi}{2A_m\gamma_{ij}\theta_{ij}k_{ij}}$             |
| $ \lambda_{ij}  \geq 1, 0 < \gamma_{ij} \leq 1$ | $\frac{\text{sign}(\lambda_{ij}) \cdot k_{ij}}{T_{ij}s + 1} e^{-\theta_{ij}s}$                       | $\frac{\pi T_{ij}}{2A_m\theta_{ij}k_{ij}}$            | $\frac{\pi}{2A_m\theta_{ij}k_{ij}}$                        |

processes with high  $D/\tau$  ratios ( $D/\tau \geq 8$ ),<sup>24</sup> where the PID controller takes the form

$$g_{c,ij}(s) = k_{c,ij} \left( 1 + \frac{1}{\tau_{i,ij}s} + \frac{\tau_{D,ij}s}{\alpha\tau_{D,ij}s + 1} \right) \quad (32)$$

**Remark 2.** If  $\lambda_{ij}$  is negative,  $\lambda_{ij} < 0$ , but  $0.15 < \beta_{ij}$ , this implies that  $u_j$  has a significant effect on  $y_i$  in the opposite direction under closed-loop control. In such a case, a controller for the loop can still be added to improve the overall system performance; however, the system integrity will be lost because of the addition of the control loop.

**Remark 3.** The significance of the proposed independent design technique is that decentralized, decoupled, and sparse control schemes can all be treated under a unified framework. The transformation between schemes is simply realized by adding or reducing the independent control loops.

## 5. Case Study

In this section, the proposed control design technique is applied to three typical industrial processes. Example 1 is employed to show that decoupling control provides better performance than decentralized control for a  $2 \times 2$  process, whereas examples 2 and 3 show that sparse control has obvious advantages over the decentralized control structure.

**Example 1.** Consider the Wood and Berry process (1973)<sup>25</sup>

$$\mathbf{G}(s) = \begin{bmatrix} \frac{12.8e^{-s}}{16.7s + 1} & \frac{-18.9e^{-3s}}{21s + 1} \\ \frac{6.6e^{-7s}}{10.9s + 1} & \frac{-19.4e^{-3s}}{14.4s + 1} \end{bmatrix}$$

The RGA ( $\Lambda$ ), normalized gain matrix ( $\mathbf{K}_N$ ), RGA ( $\Lambda_N$ ), and RARTA ( $\Gamma$ ) can be calculated, respectively, as

$$\Lambda = \begin{bmatrix} 2.0094 & -1.0094 \\ -1.0094 & 2.0094 \end{bmatrix}$$

$$\mathbf{K}_N = \begin{bmatrix} 0.7232 & -0.7875 \\ 0.3687 & -1.1149 \end{bmatrix}$$

$$\Lambda_N = \begin{bmatrix} 1.5628 & -0.5628 \\ -0.5628 & 1.5628 \end{bmatrix}$$

$$\Gamma = \begin{bmatrix} 0.7778 & 0.5576 \\ 0.5576 & 0.7778 \end{bmatrix}$$

The best pairing solution is 1–1/2–2, according to the RGA–NI–RGA rules.

The index matrix  $\mathbf{B}$  is then calculated as

$$\mathbf{B} = \begin{bmatrix} 1.0000 & 0.3601 \\ 0.3601 & 1.0000 \end{bmatrix}$$

For comparison, the gain and phase margins for all loops are specified as  $A_{m,i} = 4$  db and  $\Phi_{m,i} = 3\pi/8$  rad, respectively.

**Decentralized Control.** Because  $\lambda_{ii} > 1$  and  $\gamma_{ii} < 1$  for  $i = 1, 2$ , the original transfer functions are used for controller design, that is

$$\begin{aligned} \hat{g}_{11}(s) &= g_{11}(s) = \frac{12.8}{16.7s + 1} e^{-s} \\ \hat{g}_{22}(s) &= g_{22}(s) = \frac{-19.4e^{-3s}}{14.4s + 1} \end{aligned}$$

The decentralized controller is obtained as

$$\mathbf{G}_{c\_decentralized}(s) = \begin{bmatrix} 0.5123 + \frac{0.03068}{s} & 0 \\ 0 & -0.09716 + \frac{-0.006747}{s} \end{bmatrix}$$

**Decoupling Control.** Because  $\beta_{12} = \beta_{21} > 0.15$ , the interaction between loops cannot be ignored according to the proposed criterion.  $g_{c,12}$  and  $g_{c,21}$  should be added to the above decentralized control to make it a full decoupling control structure to obtain better performance.

The ETFs of  $g_{12}$  and  $g_{21}$  are calculated as

$$\begin{aligned} \hat{g}_{12}(s) &= \frac{18.9}{21s + 1} e^{-3s} \\ \hat{g}_{21}(s) &= \frac{-6.6}{10.9s + 1} e^{-7s} \end{aligned}$$

The resulting controllers are

$$\begin{aligned} g_{c,12}(s) &= -0.09265 + \frac{-0.0085}{s} \\ g_{c,21}(s) &= 0.1468 + \frac{0.006926}{s} \end{aligned}$$

Upon addition of these controllers to the decentralized controller matrix, the full decoupling controller is obtained as

$$\mathbf{G}_{c\_decoupling}(s) = \begin{bmatrix} 0.5123 + \frac{0.03068}{s} & -0.09265 + \frac{-0.0085}{s} \\ 0.1468 + \frac{0.006926}{s} & -0.09716 + \frac{-0.006747}{s} \end{bmatrix}$$

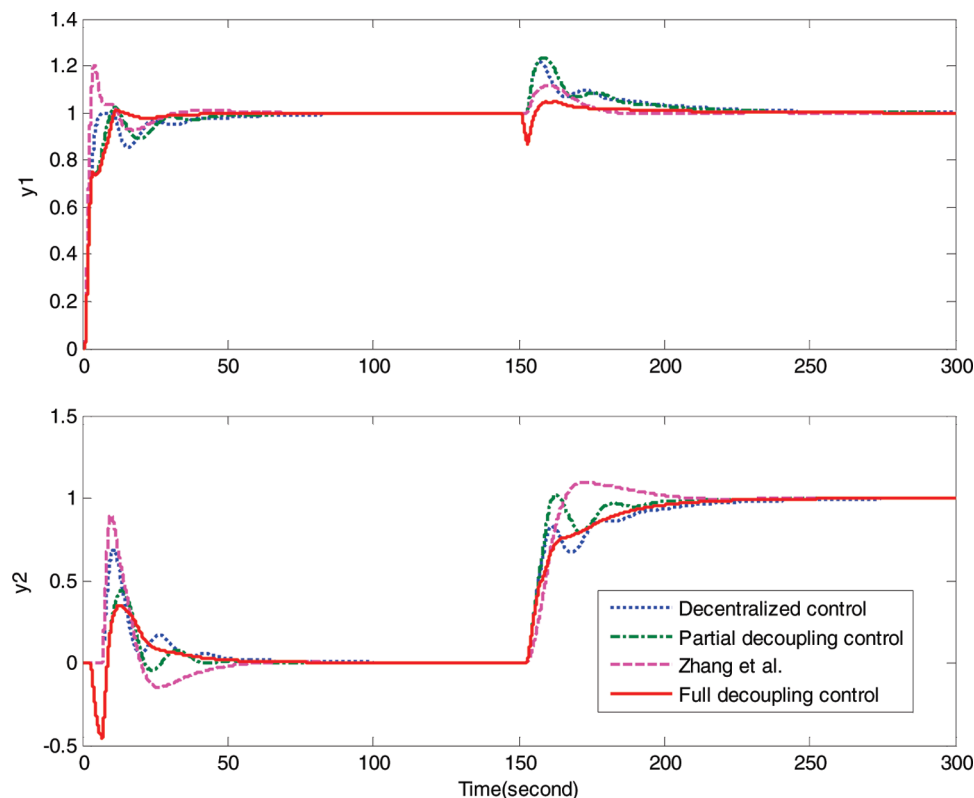


Figure 3. Step responses of WB process.

The step responses under three different control structures are given in Figure 3. For comparison, the simulation results of Zhang et al.<sup>26</sup> are also presented. This figure shows that full decoupling control results in better overall performance than can be obtained with decentralized and partial decoupling control, due to the fact that  $0.15 < \beta_{12} = \beta_{21} < 8$ . Because  $\lambda_{12} = \lambda_{21} = -1.0094 < 0$ , however, the system integrity will be lost. Indeed, if the  $u_1$ - $y_1$  loop is placed in manual control mode while the other control loops are unchanged, the system becomes unstable.

**Example 2.** Consider a  $3 \times 3$  process given by Ogunnaike and Ray (1979)<sup>27</sup>

$$G(s) = \begin{bmatrix} \frac{0.66}{6.7s+1}e^{-2.6s} & \frac{-0.61}{8.64s+1}e^{-3.5s} & \frac{-0.0049}{9.06s+1}e^{-s} \\ \frac{1.11}{3.25s+1}e^{-6.5s} & \frac{-2.36}{5s+1}e^{-3s} & \frac{-0.01}{7.09s+1}e^{-1.2s} \\ \frac{-34.68}{8.15s+1}e^{-9.2s} & \frac{46.2}{10.9s+1}e^{-9.4s} & \frac{0.87(11.61s+1)}{(3.89s+1)(18.8s+1)}e^{-s} \end{bmatrix}$$

Using the least-squares method,<sup>21</sup> the second-order plus dead time (SOPDT) element  $g_{33}(s)$  can be simplified to

$$g_{33}(s) = \left[ \frac{0.87(11.61s+1)}{(3.89s+1)(18.8s+1)}e^{-s} \right] \approx \frac{0.7922}{7.936s+1}e^{-0.465s}$$

For control system design, the original transfer function matrix becomes

$$\tilde{G}(s) = \begin{bmatrix} \frac{0.66}{6.7s+1}e^{-2.6s} & \frac{-0.61}{8.64s+1}e^{-3.5s} & \frac{-0.0049}{9.06s+1}e^{-s} \\ \frac{1.11}{3.25s+1}e^{-6.5s} & \frac{-2.36}{5s+1}e^{-3s} & \frac{-0.01}{7.09s+1}e^{-1.2s} \\ \frac{-34.68}{8.15s+1}e^{-9.2s} & \frac{46.2}{10.9s+1}e^{-9.4s} & \frac{0.7922}{7.936s+1}e^{-0.465s} \end{bmatrix}$$

The RGA ( $\Lambda$ ), normalized gain matrix ( $K_N$ ), RGA ( $\Lambda_N$ ), RARTA ( $\Gamma$ ), and index matrix  $B$  are calculated, respectively, as:

$$\Lambda = \begin{bmatrix} 2.0445 & -0.7149 & -0.3296 \\ -0.6275 & 1.8329 & -0.2055 \\ -0.4170 & -0.1180 & 1.5351 \end{bmatrix}$$

$$K_N = \begin{bmatrix} 0.0710 & -0.0502 & -0.0005 \\ 0.1138 & -0.2950 & -0.0012 \\ -1.9988 & 2.2759 & 0.0943 \end{bmatrix}$$

$$\Lambda_N = \begin{bmatrix} 1.4827 & -0.3485 & -0.1342 \\ -0.3443 & 1.407 & -0.0614 \\ -0.1384 & -0.0572 & 1.1956 \end{bmatrix}$$

$$\Gamma = \begin{bmatrix} 0.7252 & 0.4875 & 0.4071 \\ 0.5488 & 0.7669 & 0.2988 \\ 0.3318 & 0.4845 & 0.7788 \end{bmatrix}$$

$$B = \begin{bmatrix} 1 & 0.2395 & 0.0952 \\ 0.2434 & 1 & 0.0460 \\ 0.1211 & 0.0501 & 1 \end{bmatrix}$$

For comparison, three different control structures are adopted, and the gain and phase margins for all loops are specified as  $A_{m,i} = 4$  db and  $\Phi_{m,i} = 3\pi/8$  rad, respectively.

**Decentralized Control.** According to the adjustment rules, the original transfer functions are selected to be the ETFs

$$\begin{aligned} \hat{g}_{11}(s) &= g_{11}(s) = \frac{0.66}{6.7s+1}e^{-2.6s} \\ \hat{g}_{22}(s) &= g_{22}(s) = \frac{-2.36}{5s+1}e^{-3s} \\ \hat{g}_{33}(s) &= g_{33}(s) = \frac{0.7922}{7.936s+1}e^{-0.465s} \end{aligned}$$

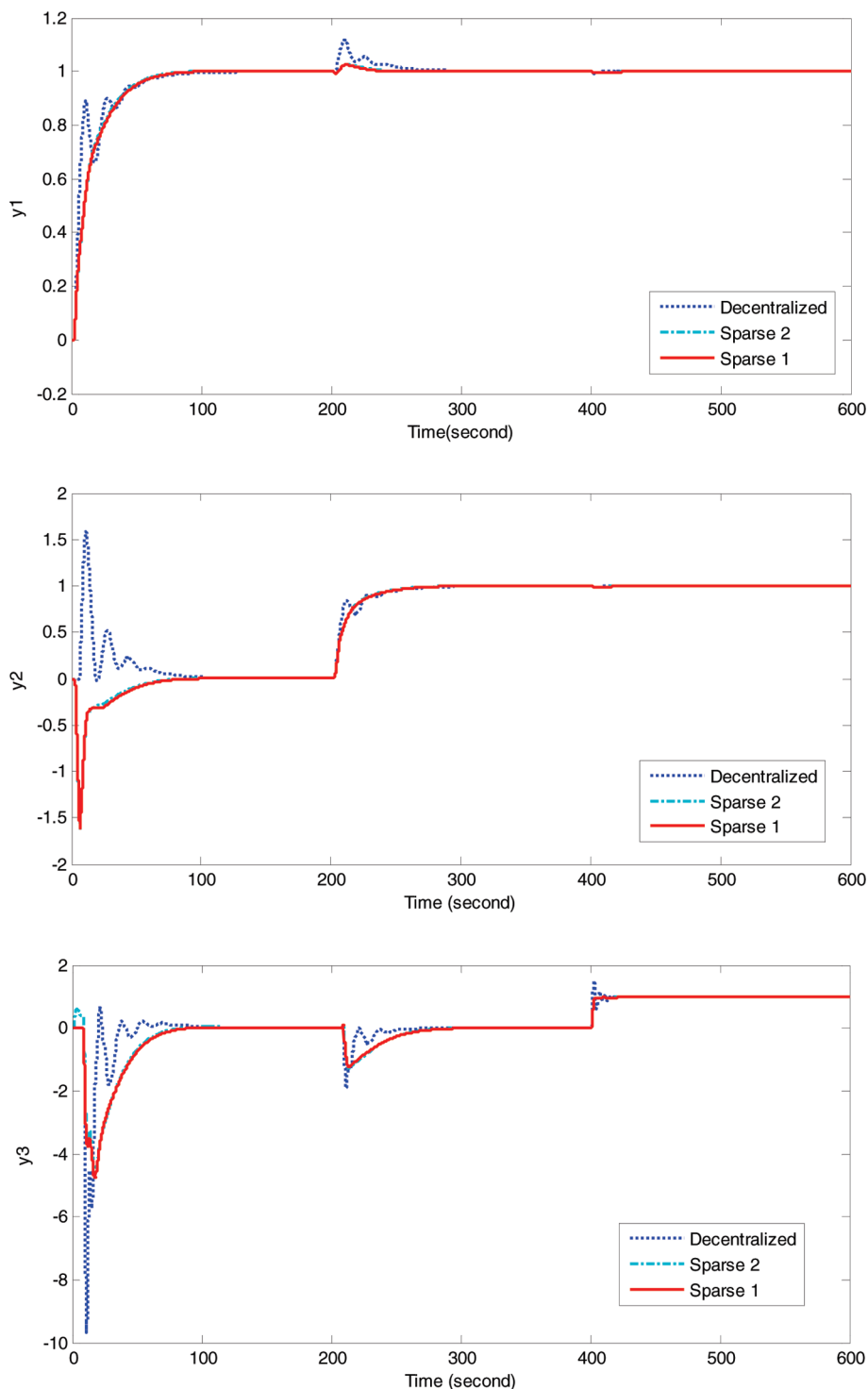


Figure 4. Step response of OR process.

The corresponding decentralized controller is obtained as

$$\mathbf{G}_{c\_decentralized}(s) = \begin{bmatrix} 1.533 + \frac{0.2288}{s} & 0 & 0 \\ 0 & -0.2773 + \frac{-0.05547}{s} & 0 \\ 0 & 0 & 8.4601 + \frac{1.066}{s} \end{bmatrix}$$

**Sparse Control 1.** According to the structure selection criterion in eq 17, sparse control should have the following structure

$$\mathbf{G}_{c\_sparse1}(s) = \begin{bmatrix} g_{c,11} & g_{c,12} & 0 \\ g_{c,21} & g_{c,22} & 0 \\ 0 & 0 & g_{c,33} \end{bmatrix}$$

The ETFs for the off-diagonal elements are

$$\begin{aligned} \hat{g}_{12}(s) &= \frac{0.8533}{8.64s + 1} e^{-3.5s} \\ \hat{g}_{21}(s) &= \frac{-1.7691}{3.25s + 1} e^{-6.5s} \end{aligned}$$

Adding the two off-diagonal controllers, the sparse controllers are obtained as

$$\mathbf{G}_{\text{c\_sparse1}}(s) = \begin{bmatrix} 1.533 + \frac{0.2288}{s} & -0.111 + \frac{-0.03415}{s} & 0 \\ 1.136 + \frac{0.1315}{s} & -0.2773 + \frac{-0.05547}{s} & 0 \\ 0 & 0 & 8.4601 + \frac{1.066}{s} \end{bmatrix}$$

### Sparse Control 2.

Adding two more controllers that have relatively large  $\beta$  values, we obtain the control structure of

$$\mathbf{G}_{\text{c\_sparse2}}(s) = \begin{bmatrix} g_{c,11} & g_{c,12} & g_{c,13} \\ g_{c,21} & g_{c,22} & 0 \\ g_{c,31} & 0 & g_{c,33} \end{bmatrix}$$

and for  $|\lambda_{13}| < 1$ ,  $\gamma_{13} < 1$ , and  $|\lambda_{31}| < 1$ ,  $\gamma_{31} < 1$ , the ETFs of  $g_{13}$  and  $g_{31}$  are

$$\begin{aligned} \hat{g}_{13}(s) &= \frac{0.0149}{9.06s + 1} e^{-s} \\ \hat{g}_{31}(s) &= \frac{83.1630}{8.15s + 1} e^{-9.2s} \end{aligned}$$

The final controller has the form

$$\mathbf{G}_{\text{c\_sparse2}}(s) = \begin{bmatrix} 1.533 + \frac{0.2288}{s} & -0.111 + \frac{-0.03415}{s} & 0.004183 + \frac{0.0005133}{s} \\ 1.136 + \frac{0.1315}{s} & -0.2773 + \frac{-0.05547}{s} & 0 \\ 2.624 + \frac{0.2896}{s} & 0 & 8.4601 + \frac{1.066}{s} \end{bmatrix}$$

The results of the closed-loop step responses under the three control structures are given in Figure 4.

The simulation results reveal the following: (1) Sparse control indeed provides a great improvement in performance compared with decentralized control. (2) The closed-loop performance shows no improvement upon addition of additional loops that do not meet the structure selection criterion.

### Example 3.

Consider a  $4 \times 4$  process given by Alatiqi (1985)<sup>28</sup>

$$\mathbf{G}(s) = \begin{bmatrix} \frac{4.09e^{-1.3s}}{(33s+1)(8.3s+1)} & \frac{-6.36e^{-0.2s}}{(31.6s+1)(20s+1)} & \frac{-0.25e^{-0.4s}}{21s+1} & \frac{-0.49e^{-5s}}{(22s+1)^2} \\ \frac{-4.17e^{-4s}}{45s+1} & \frac{6.93e^{-1.01s}}{44.6s+1} & \frac{-0.05e^{-5s}}{(34.5s+1)^2} & \frac{1.53e^{-2.8s}}{48s+1} \\ \frac{-1.73e^{-17s}}{(13s+1)^2} & \frac{5.11e^{-11s}}{(13.3s+1)^2} & \frac{4.61e^{-1.02s}}{18.5s+1} & \frac{-5.48e^{-0.5s}}{15s+1} \\ \frac{-11.18e^{-2.6s}}{(43s+1)(6.5s+1)} & \frac{14.04e^{-0.02s}}{(45s+1)(10s+1)} & \frac{-0.1e^{-0.05s}}{(31.6s+1)(5s+1)} & \frac{4.49e^{-0.6s}}{(48s+1)(6.3s+1)} \end{bmatrix}$$

The RGA ( $\mathbf{\Lambda}$ ), normalized gain matrix ( $\mathbf{K}_N$ ), RNGA ( $\mathbf{\Lambda}_N$ ), and RARTA ( $\mathbf{\Gamma}$ ) can be calculated, respectively, as

$$\begin{aligned} \mathbf{\Lambda} &= \begin{bmatrix} 3.1058 & -0.9007 & -0.4749 & -0.7302 \\ -5.0308 & 4.6742 & -0.0395 & 1.3961 \\ -0.0838 & 0.0543 & 1.5492 & -0.5197 \\ 3.0088 & -2.8278 & -0.0348 & 0.8538 \end{bmatrix} \\ \mathbf{K}_N &= \begin{bmatrix} 0.2808 & -0.2575 & -0.0117 & -0.0181 \\ -0.0851 & 0.1519 & -0.0013 & 0.0301 \\ -0.0577 & 0.2103 & 0.2362 & -0.3535 \\ -0.8047 & 0.8570 & -0.0115 & 0.3825 \end{bmatrix} \\ \mathbf{\Lambda}_N &= \begin{bmatrix} 1.8033 & -0.4423 & -0.1774 & -0.1836 \\ -1.0320 & 2.2582 & 0.0291 & -0.2553 \\ -0.0212 & 0.0246 & 1.2330 & -0.2364 \\ 0.2498 & -0.8405 & -0.0847 & 1.6754 \end{bmatrix} \\ \mathbf{\Gamma} &= \begin{bmatrix} 0.5806 & 0.4910 & 0.3736 & 0.2515 \\ 0.2051 & 0.4831 & -0.7361 & -0.1829 \\ 0.2530 & 0.4523 & 0.7959 & 0.4549 \\ 0.0830 & 0.2972 & 2.4314 & 1.9622 \end{bmatrix} \end{aligned}$$



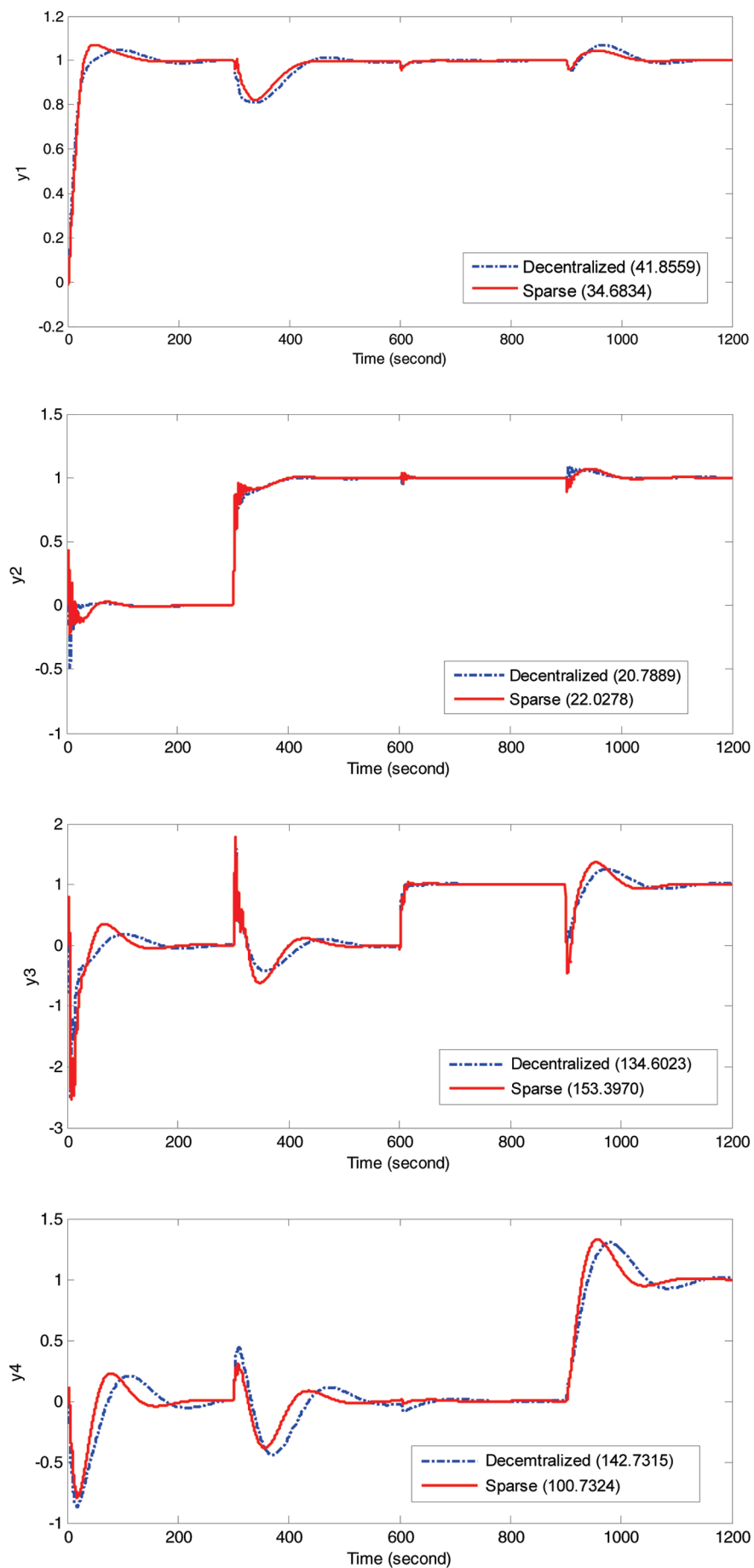


Figure 5. Response and IAE values of A2 process.

According to the pairing rules, this is a diagonal pairing (i.e., the loops should be paired as 1–1, 2–2, 3–3, and 4–4), and the index matrix  $\mathbf{B} = [\beta_{ij}]_{n \times n}$  is calculated as

$$\mathbf{B} = \begin{bmatrix} 1.0000 & 0.2452 & 0.0984 & 0.1018 \\ 0.4570 & 1.0000 & 0.0129 & 0.1131 \\ 0.0172 & 0.0199 & 1.0000 & 0.1917 \\ 0.1491 & 0.5017 & 0.0505 & 1.0000 \end{bmatrix}$$

### Decentralized Control.

According to the adjustment rules, the ETFs of the diagonal transfer functions are calculated as

$$\begin{aligned} \hat{g}_{11}(s) &= \frac{4.09e^{-1.3s}}{273.9s^2 + 41.3s + 1} \\ \hat{g}_{22}(s) &= \frac{6.93e^{-1.01s}}{44.6s + 1} \\ \hat{g}_{33}(s) &= \frac{4.61e^{-1.02s}}{18.5s + 1} \\ \hat{g}_{44}(s) &= \frac{5.2588}{302.4s^2 + 27.6730s + 1} e^{-1.1773s} \end{aligned}$$

The decentralized controller is designed using the gain and phase method ( $A_{m,i} = 4$  db) as

$$\mathbf{G}_{c\_decentralized}(s) = \begin{bmatrix} 3.0503 + \frac{0.0739}{s} + 20.2295s & 0 & 0 & 0 \\ 0 & 2.502 + \frac{0.05611}{s} & 0 & 0 \\ 0 & 0 & 1.545 + \frac{0.08351}{s} & 0 \\ 0 & 0 & 0 & 1.7530 + \frac{0.0634}{s} + 19.1809 \end{bmatrix}$$

### Sparse Control.

Because  $\beta_{12} > 0.15$ ,  $\beta_{21} > 0.15$ ,  $\beta_{42} > 0.15$ , and  $\beta_{34} > 0.15$ , the sparse control structure should include  $g_{c,21}$ ,  $g_{c,12}$ ,  $g_{c,24}$ , and  $g_{c,43}$  loops. The ETFs for these transfer functions are obtained, respectively, as

$$\begin{aligned} \hat{g}_{12} &= \frac{(-6.36/-0.9007)e^{-0.2s}}{(31.6s + 1)(20s + 1)} = \frac{7.0612e^{-0.2s}}{(31.6s + 1)(20s + 1)} \\ \hat{g}_{21} &= \frac{(-4.17/-1)e^{-4s}}{45s + 1} = \frac{4.17e^{-4s}}{45s + 1} \\ \hat{g}_{42} &= \frac{(14.04/-1)e^{-0.02s}}{(45s + 1)(10s + 1)} = \frac{-14.04e^{-0.02s}}{(45s + 1)(10s + 1)} \\ \hat{g}_{34} &= \frac{(-5.48/-0.5197)e^{-0.5s}}{15s + 1} = \frac{10.5445e^{-0.5s}}{15s + 1} \end{aligned}$$

Considering the high  $D/\tau$  ratios of the above four ETFs, the off-diagonal controllers are designed by the IMC–Maclaurin method. The sparse controllers are then obtained as

$$\mathbf{G}_{c\_sparse}(s) = \begin{bmatrix} 3.0503 + \frac{0.0739}{s} + 20.2295s & 1.2227\left(1 + \frac{0.02176}{s} + \frac{0.8628s}{8.631s + 1}\right) & 0 & 0 \\ 0.6824\left(1 + \frac{0.02037}{s} + \frac{10.4103s}{10.14s + 1}\right) & 2.502 + \frac{0.05611}{s} & 0 & -0.3732\left(1 + \frac{0.0190}{s} + \frac{8.1913s}{64.95s + 1}\right) \\ 0 & 0 & 1.545 + \frac{0.08351}{s} & 0 \\ 0 & 0 & 0.4074\left(1 + \frac{0.0665}{s} + \frac{0.0353s}{3.532s + 1}\right) & 1.7530 + \frac{0.0634}{s} + 19.1809 \end{bmatrix}$$

The results of the closed-loop step response and integral absolute error (IAE) values are given in Figure 5.

It can be seen that the overall performance of sparse control is superior.

## 6. Conclusion

In this work, by introducing the concepts of interaction index, equivalent transfer function, and independent design, we have presented a systematic design approach for multivariable processes. The structure selection criterion provides a compromise between system performance and structural complexity, whereas the equivalent transfer function and independent design make the conversion between decentralized, decoupling, and sparse control schemes possible simply through the addition or removal of loop controllers. This method is very easy to understand and implement. The simulation results for several industrial processes show that the selected

control structure provides overall better system performance than other structures. Further research will focus on the stability and robustness analysis of sparse control. This topic is currently under investigation and will be reported later.

## Literature Cited

- (1) Luyben, W. L. Simple method for tuning SISO controllers in multivariable systems. *Ind. Eng. Chem. Process Des. Dev.* **1986**, *25*, 654.
- (2) Xiong, Q.; Cai, W. J.; He, M. J.; He, M. Decentralized control system design for multivariable processes—A novel method based on effective relative gain array. *Ind. Eng. Chem. Res.* **2006**, *45*, 2769.
- (3) Åström, K. J.; Johansson, K. H.; Wang, Q. G. Design of decoupled PI controllers for two-by-two systems. *IEE Proc. Control Theory Appl.* **2002**, *149*, 74.
- (4) Loh, A. P.; Hang, C. C.; Quek, C. K.; Vasnani, V. U. Autotuning of multiloop proportional–integral controllers using relay feedback. *Ind. Eng. Chem. Res.* **1993**, *32*, 1102.
- (5) Shen, S. H.; Yu, C. C. Use of relay-feedback test for autotuning of multivariable systems. *AIChE J.* **1994**, *40*, 627.
- (6) Xiong, Q.; Cai, W. J. Effective transfer function method for decentralized control system design of multi-input multi-output processes. *J. Process Control* **2006**, *16*, 773.
- (7) Huang, H. P.; Jeng, J. C.; Chiang, C. H.; Pan, W. A direct method for multi-loop PI/PID controller design. *J. Process Control* **2003**, *13*, 769.
- (8) Luyben, W. L. Distillation decoupling. *AIChE J.* **1970**, *16*, 198.
- (9) Shinskey, F. G. *Process Control Systems: Application, Design and Adjustment*; McGraw-Hill: New York, 1988.
- (10) Gagnon, E.; Pomerleau, A.; Desbiens, A. Simplified, ideal or inverted decoupling. *ISA Trans.* **1998**, *37*, 265.
- (11) Yang, Y. S.; Wang, Q. G.; Wang, L. P. Decoupling control design via linear matrix inequalities. *IEE Proc. Control Theory Appl.* **2005**, *152*, 357.
- (12) Wang, Q. G.; Huang, B.; Guo, X. Auto-tuning of TITO decoupling controllers from step tests. *ISA Trans.* **2000**, *39*, 407.
- (13) Wang, Q. G.; Zou, B.; Lee, T. H.; Bi, Q. Auto-tuning of multivariable PID controllers from decentralized relay feedback. *Automatica* **1997**, *33*, 319.
- (14) Cai, W. J.; Ni, W.; He, M. J.; Ni, C. Y. Normalized decoupling—A new approach for MIMO process control system design. *Ind. Eng. Chem. Res.* **2008**, *47*, 7347.
- (15) Shen, Y. L.; Cai, W. J.; Li, S. Y. Normalized decoupling control for high dimensional MIMO processes with application to room temperature control of HVAC systems. *Control Eng. Pract.*, manuscript submitted.
- (16) Wonham, W. M.; Morse, A. S. Decoupling and pole assignment in linear multivariable systems: A geometric approach. *SIAM J. Control* **1970**, *8*, 1.
- (17) Zhang, W. Z.; BAO, J.; Lee, P. L. Control structure selection based on block-decentralized integral controllability. *Ind. Eng. Chem. Res.* **2003**, *42*, 5152.
- (18) Commault, C.; Dion, J. M. Transfer matrix approach to the triangular block decoupling problem. *Automatica* **1983**, *19*, 533.
- (19) Salgado, M. E.; Conley, A. MIMO interaction measure and controller structure selection. *Int. J. Control* **2004**, *77*, 367.
- (20) He, M. J.; Cai, W. J.; Ni, W.; Xie, L. H. RGA based control system configuration for multivariable processes. *J. Process Control* **2009**, *19*, 1036.
- (21) Xiong, Q.; Cai, W. J.; He, M. J. Equivalent transfer function method for PI/PID controller design of MIMO processes. *J. Process Control* **2007**, *17*, 665.
- (22) Skogestad, S. Simple analytic rules for model reduction and PID controller tuning. *J. Process Control* **2003**, *13*, 291.
- (23) Bi, Q.; Cai, W. J.; Lee, E. L.; Wang, Q. G.; Hang, C. C. Robust identification of first-order plus dead-time model from step response. *Control Eng. Pract.* **1999**, *7*, 71.
- (24) Panda, R. C.; Yu, C. C.; Huang, H. P. PID tuning rules for SOPDT systems: Review and some new results. *ISA Trans.* **2004**, *43*, 283.
- (25) Wood, R. K.; Berry, M. W. Terminal composition control of a binary distillation column. *Chem. Eng. Sci.* **1973**, *28*, 1707.
- (26) Zhang, Y.; Wang, Q. G.; Astrom, K. J. Dominant pole placement for multi-loop control systems. *Automatica* **2002**, *38*, 1213.
- (27) Ogunnaike, B. A.; Ray, W. H. Multivariable controller design for linear systems having multiple time delays. *AIChE J.* **1979**, *25*, 1043.
- (28) Alatiqi I. Composition control of distillation systems separating ternary mixtures with small intermediate feed concentrations. Ph.D. Thesis, Lehigh University, Bethlehem, PA, 1985.

Received for review September 15, 2009

Revised manuscript received October 23, 2009

Accepted November 2, 2009

IE901453Z